



# Preparation and characterization of nano TiO<sub>2</sub>/micron Cr<sub>2</sub>O<sub>3</sub> composite particles

Bin Wang\*, Jun Yan, Haiping Cui, Shiguo Du

Shijiazhuang Mechanical Engineering College, No. 97, He Ping South Road, Shijiazhuang, Hebei Province 050003 China

## ARTICLE INFO

### Article history:

Received 17 October 2010

Received in revised form 27 January 2011

Accepted 2 February 2011

Available online 26 February 2011

### Keywords:

TiO<sub>2</sub> nanoparticles  
Composite particles  
Absorption intensity

## ABSTRACT

Nano-TiO<sub>2</sub>/micro-size Cr<sub>2</sub>O<sub>3</sub> composite particles were first prepared by hydrolysis of Ti(OBu)<sub>4</sub> in an abundant acidic aqueous solution without calcinations at room temperature. XPS analysis shows that the element C, O, Ti and Sn existed on the surfaces of the composite particles. Observation by field emission scanning electronic microscope shows TiO<sub>2</sub> particles of 10–15 nm covers on Cr<sub>2</sub>O<sub>3</sub> powder surfaces to form nanometer/micron composite particles. UV–vis spectra show a red shift of the absorption edge and a significant increase of absorption intensity in the visible region. These results confirm that TiO<sub>2</sub> of anatase type can be synthesized on the surface of Cr<sub>2</sub>O<sub>3</sub>.

© 2011 Elsevier B.V. All rights reserved.

## 1. Introduction

Since Fujishima and Honda [1] discovered the photocatalytic splitting of water on TiO<sub>2</sub> electrodes in 1972, titanium dioxide has been the subject of research as a semiconductor photocatalyst for application in solar-energy conversion and environmental purification [2–4]. Due to its specific optical and electronic properties, low cost, chemical stability and non-toxicity, titanium dioxide is an important photocatalyst with current commercial applications. However, one obstacle toward its practical application is that photocatalytic processes can only be activated by ultraviolet light, which accounts for only about 4% of the incoming solar energy. Another shortcomings of conventional powder catalysts lay difficulty in separation of catalyst after each run [5]. These disadvantages of TiO<sub>2</sub> resulted in inefficient photocatalytic activity. One way to enhance the photocatalytic activity is the coating and doping of other materials, including metal ions and semiconductors, onto the surface of TiO<sub>2</sub> nanoparticles [6–8]. The coupling of two semiconductors provides a novel approach to achieve a more efficient charge separation, an increased lifetime of the charge carriers, and the enhancement of visible light response [9,3,10,11]. Papp et al. [12–15] investigated the TiO<sub>2</sub>/Al<sub>2</sub>O<sub>3</sub>, TiO<sub>2</sub>/ZrO<sub>2</sub>, TiO<sub>2</sub>/WO<sub>3</sub> and TiO<sub>2</sub>/MoO<sub>3</sub> systems and Langlet et al. [16] have recently published results on TiO<sub>2</sub>-coated polystyrene spheres. Much attention has been paid on the studies of TiO<sub>2</sub> composite nanoparticles, but little is focused on the preparation and characteristic of nano-TiO<sub>2</sub> coating micro-size particles. In addition, the synthesis condition

of TiO<sub>2</sub>-based catalysts is usually harsh, for example, needs high temperature or high pressure. The calcination process is usually necessary for the preparation of TiO<sub>2</sub>.

In this study, we prepared nano-TiO<sub>2</sub>/micro Cr<sub>2</sub>O<sub>3</sub> by hydrolysis of Ti(OBu)<sub>4</sub> in an abundant acidic aqueous solution at room temperature. The as prepared samples were characterized by XPS, SEM, Raman spectrum, XRD and UV–vis. The results shows that the structure of TiO<sub>2</sub> loaded on the surface of Cr<sub>2</sub>O<sub>3</sub> powder is mainly of anatase type which have high catalytic activity. There is a red shift of the absorption edge and a significant increase of absorption intensity in the visible region. How to load the photo-catalyst uniformly and firmly on carriers under mild conditions, keeping high catalytic activity and meeting specific physics and chemistry performance and making the catalyst easy to recycling is the difficult points of current studies.

## 2. Experimental

### 2.1. Preparation of the catalysts

Samples were prepared according to the following process. 5 g Cr<sub>2</sub>O<sub>3</sub> powder was put into flask, then 0.3 g SnCl<sub>4</sub>·H<sub>2</sub>O and 40 ml C<sub>2</sub>H<sub>5</sub>OH were added. 3 ml Ti(OBu)<sub>4</sub> were dissolved in 20 ml C<sub>2</sub>H<sub>5</sub>OH, and then 6 ml H<sub>2</sub>O was added with vigorous stirring. Hydrochloric acid was then added in order to dissolve the precipitate forming limpid yellow sol. Poured the sol into the flask with Cr<sub>2</sub>O<sub>3</sub> powders, the mixture was refluxed at 80 °C for 50 min. After that, the prepared samples were washed several times carefully with anhydrous ethanol and distilled water. The idling samples were made by refluxing directly the sol without Cr<sub>2</sub>O<sub>3</sub>.

### 2.2. Characterization

The phases presented in the as-prepared particles, its chemical composition, and morphology were determined by X-ray diffraction (XRD; Rigaku RAD-C; Cu-Kα, 40 kV, 30 mA), X-ray photoelectron spectroscopy (XPS; ESCA System; PHI1600X), along with field emission scanning electron microscopy (FE-SEM; XL30S-FEG),

\* Corresponding author.

E-mail address: [wang.bin52@163.com](mailto:wang.bin52@163.com) (B. Wang).

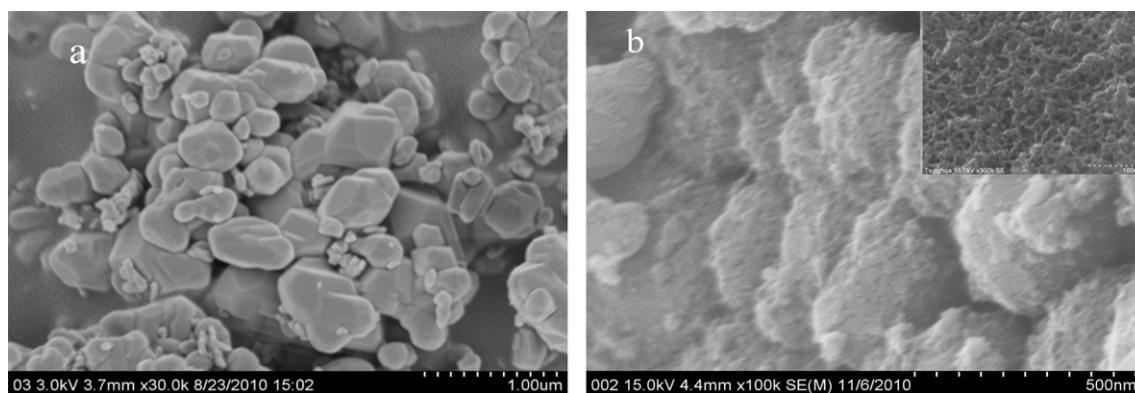


Fig. 1. SEM micrographs of (a) naked chromic oxide and (b) titania-coated chromic oxide.

respectively. The absorption edge of the samples was measured using a UV–vis spectrophotometer (Perkin Elmer–Lambda 35 UV–vis Spectrometer), and  $\text{BaSO}_4$  was used as the reflectance standard in a UV–vis diffuse reflectance experiment.

### 3. Results and discussion

#### 3.1. Morphology of $\text{TiO}_2$ – mounted chromic oxide

Fig. 1 illustrates the SEM micrographs of  $\text{TiO}_2/\text{Cr}_2\text{O}_3$  composite particles and naked  $\text{Cr}_2\text{O}_3$ . The results show that the naked  $\text{Cr}_2\text{O}_3$  particles are smooth and irregularly shaped with the sizes below  $1\ \mu\text{m}$ . After coating process,  $\text{TiO}_2$  nanoparticles were formed on the surfaces of chromic oxide, as shown in Fig. 1b. The inserted image in Fig. 1b shows that  $\text{TiO}_2$  particles are evenly distributed on the surfaces without aggregation, and the size of the  $\text{TiO}_2$  is about 10–15 nm. It is proved from the results that nano  $\text{TiO}_2$ /micro  $\text{Cr}_2\text{O}_3$  composite particles have been prepared.

#### 3.2. XPS analysis

Fig. 2 shows the XPS results of the particles. The peaks of C1s, O1s, Ti2p, Sn3d and Cr2p appeared on the surface of the composite particles, showing that the surface mainly contained elements of C, O, Ti, Sn and Cr. Among them, the element of C was the residuum created by organic rough material. The results show that the binding energy of Ti2p, Sn3d and Cr2p peaks were 459 eV, 486 eV and 580 eV, separately.

Due to the spinning–rail coupling of the electron, the energy level of Ti2p was broken to two levels marked as  $\text{Ti}2p_{1/2}$  and  $\text{Ti}2p_{3/2}$ ,  $\text{Ti}2p_{3/2}$  and  $\text{Ti}2p_{1/2}$  located at 458.7 and 464.5 eV (Fig. 3a), respectively. The proportion of the two peaks zone was about 0.5 and

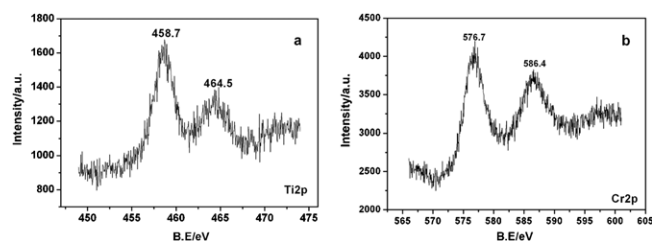


Fig. 3. Spectra of Ti element and Cr element on sample.

the  $D$ -value was about 5.8, which was coincident with the reference [17]. The  $\text{Ti}2p_{3/2}$  binding energy exceeds that of Ti metal (454.0 eV), TiO (455.0 eV), and  $\text{Ti}_2\text{O}_3$  (456.7 eV), but is similar to that of  $\text{TiO}_2$  (458.4–458.7 eV), which suggests that Ti is in the +4 oxidation state and directly bonded to oxygen. At the same time, for the as-deposited composite particles, Fig. 3b shows the existence of chromic oxide: the binding energy of  $\text{Cr}2p$  located at 576.7 and 586.4 eV corresponding to that of  $\text{Cr}2p_{3/2}$ , the possible reason for which is that the thickness of  $\text{TiO}_2$  film is very thin, so chromic oxide under it can be detected.

#### 3.3. X-ray diffraction

The XRD patterns of nano  $\text{TiO}_2/\text{Cr}_2\text{O}_3$  are shown in Fig. 4. By careful observation, it can be found that peaks emerge at  $2\theta = 24.5, 33.6, 36.2, 41.5, 44.1$  and  $54.3$ , which indicates that the structure of  $\text{Cr}_2\text{O}_3$  was mainly green chrome ore. The analysis of the diffraction peaks of composite particles reveals the presence of  $\text{Cr}_2\text{O}_3$ , while no obvious peaks indicating the existence of  $\text{TiO}_2$ . The rea-

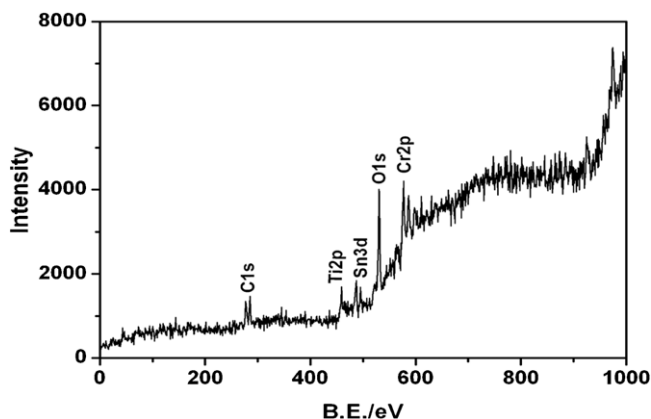


Fig. 2. XPS of the compound powders.

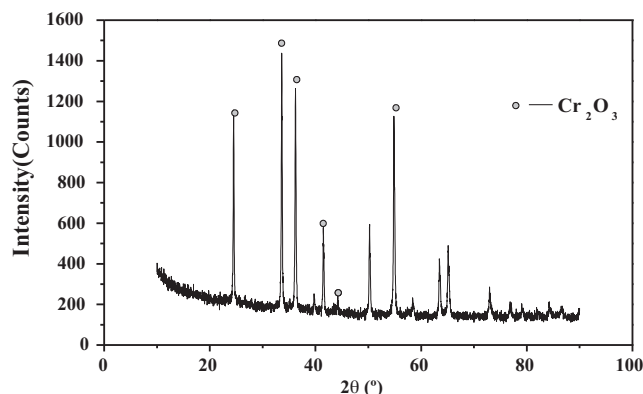


Fig. 4. XRD of the  $\text{TiO}_2/\text{Cr}_2\text{O}_3$  compound powders.

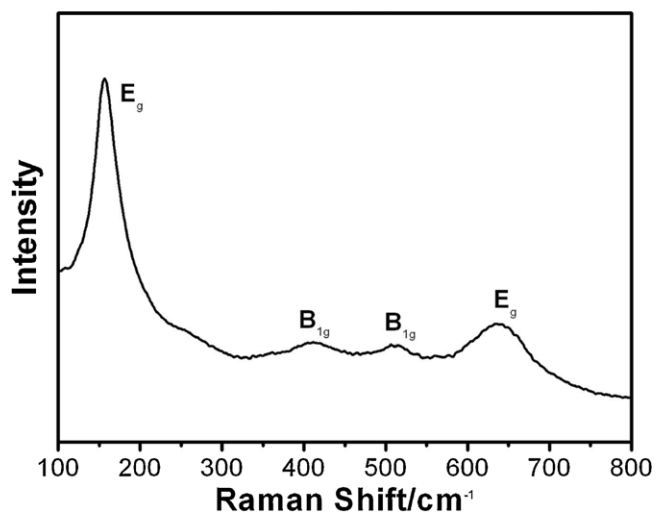


Fig. 5. Raman spectra of idling samples.

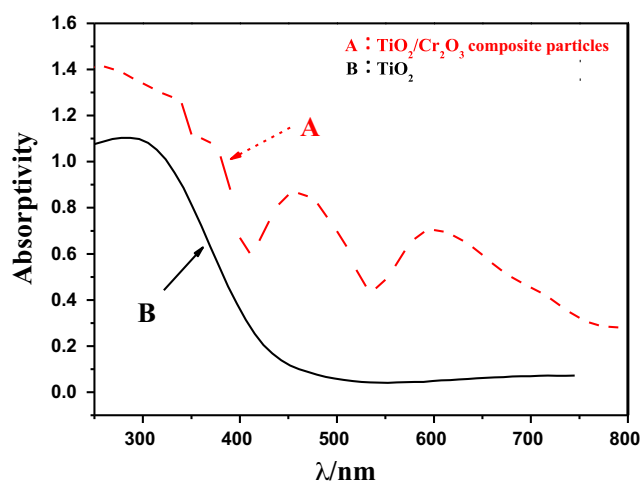


Fig. 6. UV-vis spectrum of the  $\text{TiO}_2/\text{Cr}_2\text{O}_3$  composite particles (A) and naked  $\text{TiO}_2$  particles (B).

son is that the concentration of the loaded  $\text{TiO}_2$  particles is very low (less than 5%). XRD cannot detect components with such low contents [18].

#### 3.4. Raman analysis of idling samples

In order to confirm the crystal structure of  $\text{TiO}_2$ , we carry on Raman spectrum for the idling samples. The results were showed in Fig. 5. The characteristic peaks appeared at 143, 392, 510 and  $633\text{ cm}^{-1}$  stand for Raman oscillating mode  $E_g(143, 633\text{ cm}^{-1})$ ,  $B_{1g}(392\text{ cm}^{-1})$  and  $B_{2g}(510\text{ cm}^{-1})$  separately, which can confirm that the structure of  $\text{TiO}_2$  loaded on the surface of  $\text{Cr}_2\text{O}_3$  powder is mainly of anatase type [19]. The result shows that the Raman signal of the nano  $\text{TiO}_2$  particle is a little weak and obviously broadened compared with the bulk  $\text{TiO}_2$ , which is possibly due to the effects of long-range coulomb force on the phonon spectrum [20].

#### 3.5. UV-vis diffuse reflectance spectra of the composite particles

Fig. 6 shows the UV-vis diffuse reflectance spectra of the  $\text{TiO}_2/\text{Cr}_2\text{O}_3$  composite particles and  $\text{TiO}_2$ . Three absorption peaks appear at 370 nm, 460 nm and 600 nm. The absorption is extended to the wavelength of 750 nm. An obvious red shift of UV-vis reflectance spectra of  $\text{TiO}_2/\text{Cr}_2\text{O}_3$  composite nanoparticles was observed when compared with the spectrum of neat anatase  $\text{TiO}_2$  nanoparticles. This suggests that the  $\text{TiO}_2/\text{Cr}_2\text{O}_3$  composite particles have a lower band gap than the neat anatase  $\text{TiO}_2$  nanoparticles. It has been reported that the band-gap energy of  $\text{Cr}_2\text{O}_3$  and that of  $\text{TiO}_2$  were of 3.5 eV and 3.2 eV, and the wavelength of the absorption edge of  $\text{Cr}_2\text{O}_3$  and  $\text{TiO}_2$  was 357 nm and 365 nm, respectively. Therefore, the red shift of  $\text{TiO}_2/\text{Cr}_2\text{O}_3$  composite nanoparticles could be attributed to the contribution of each of the oxide component  $\text{Cr}_2\text{O}_3$  and  $\text{TiO}_2$  [21]. So the  $\text{Cr}_2\text{O}_3$  as the carrier for  $\text{TiO}_2$  extends the photo response range of composite semiconductor.

#### 4. Conclusions

Nano- $\text{TiO}_2$ /micro size  $\text{Cr}_2\text{O}_3$  composite particles was successfully synthesized without calcination by hydrolysis of  $\text{Ti}(\text{OBU})_4$  in an abundant acidic aqueous solution. The particle size of  $\text{TiO}_2$  in the composites is less than 15 nm and the  $\text{TiO}_2$  loaded on the surface of  $\text{Cr}_2\text{O}_3$  powder is mainly of anatase type. The UV absorption edge of the composites shows a red-shift as compared to that of  $\text{TiO}_2$  particles. The prepared samples show a high absorption intensity, which could be attributed to the combination effect  $\text{Cr}_2\text{O}_3$  and  $\text{TiO}_2$ .

#### Acknowledgements

This work is supported by National Nature Science Foundation of China (grant: 50842045) and Science Research Foundation of Shijiazhuang Mechanical Engineering College (grant no. YJXM08008 and JCB1006)

#### References

- [1] A. Fujishima, K. Honda, Nature 238 (53) (1972) 37–38.
- [2] A. Fujishima, T.N. Rao, D.A. Tryck, J. Photochem. Photobiol C: Photochem. Rev. 1 (2000) 1–21.
- [3] A.L. Linsebigler, G. Lu, J.T. Jr. Yates, Chem. Rev. 95 (1995) 735–758.
- [4] Taizo Sano, Nobuaki Negishi, Denis Mas, Koji Takeuchi, J. Catal. 194 (1) (2000) 71–79.
- [5] Kang S M., J. Mol. Catal. A: Chem. 197 (2003) 173–183.
- [6] H.M. Yates, M.G. Nolan, D.W. Sheel, M.E. Pemble, J. Photochem. Photobiol. A 179 (1–2) (2006) 213–223.
- [7] Y. Bessekhouad, D. Robert, J.V. Weber, N. Chaoui, J. Photochem. Photobiol. A: Chem. 167 (2004) 49–57.
- [8] A. Erkan, U. Bakir, G. Karakas, J. Photochem. Photobiol. A 184 (2006) 313–321.
- [9] A.-W. Xu, Y. Gao, H.-Q. Liu, J. Catal. 207 (2) (2002) 151–157.
- [10] O. Carp, C.L. Huisman, A. Reller, Solid State Chem. 32 (2004) 33–177.
- [11] C. Wang, J. Zhao, X. Wang, Appl. Catal. B: Environ. 39 (2002) 269–279.
- [12] S. Liao, H. Donggen, D. Yu, Y. Su, G. Yuan, J. Photochem. Photobiol. A: Chem. 168 (1–2) (2004) 7–13.
- [13] B. Pal, M. Sharon, G. Nogami, Mater. Chem. Phys. 59 (3) (1999) 254–261.
- [14] J. Papp, S. Soled, K. Dwight, et al., Chem. Mater. 6 (1994) 496–500.
- [15] C. Anderson, A. Bard, J. Phys. Chem. 101 (1997) 2611.
- [16] M. Langlet, A. Kim, M. Audier, J.-M. Herrmann, J. Sol-Gel Sci. Technol. 25 (2002) 223–234.
- [17] D. Burdeaux, P. Townsend, J. Carr, J. Electron. Mater. 19 (12) (1990) 1357–1366.
- [18] Z. Ma, S. She, S. Min, Nat. Sci. 41 (2) (2005) 64–67.
- [19] S.P.S. Porto, P.A. Fleury, T.C. Damen, Phys. Rev. 154 (1967) 522.
- [20] Y. Jun, C. Haiping, W. Bin, J. Synth. Cryst. 39 (2) (2010) 407–411.
- [21] R. Hu, S. Zhong, Chem. J. Chin. Univ. 27 (1) (2006) 134–139.